

# Special and innovative aspects of the GTC M2 Drive mechanism

Enrique García<sup>\*a</sup>, Lorenzo Zago<sup>\*\*b</sup>, Daniele Gallieni<sup>\*\*\*c</sup>  
<sup>a</sup>NTE, S.A.; <sup>b</sup>CSEM, S.A.; <sup>c</sup>ADS International srl;

## ABSTRACT

The paper presents some special, innovative and technological aspects of the secondary mirror mechanism for the GTC 10.8-m telescope, such as: The dual control loop of the hexapod actuators, which provides the GTC M2 alignment system with an absolute accuracy better than a few microns, and a resolution as low as 40 nm. The particular design of the hexapod flexure joints, which ensures frictionless joints without backlash, while effectively limiting the travel of the hexapod to the desired range only. The locking devices, based on an original rotating cam principle, which ensure the safe locking of the M2 support to the hexapod lower plate when the chopper function is not utilized. CuBe flexure parts have been manufactured by Electrodischarge Machining (EDM), and heat treated for maximum strength and fatigue load. A systematic approach to the Reliability, Maintainability and Safety aspects, aimed at ensuring the operational feasibility of the mechanism along its life cycle.

## 1. INTRODUCTION

The GTC design includes secondary mirror active drives, which must meet two mirror positioning functions:

-Active alignment in five degrees of freedom (three orthogonal lineal displacements, two rotations perpendicular to the telescope axis) to allow optical alignment to compensate for telescope tube thermal and gravitational deformations.

-Fast rotations perpendicular to the optical axis of the telescope to allow image-motion compensation – provided an external image motion sensing signal-, and multi-point chopping for background subtraction.

Table 1 summarizes the main specifications of the subsystem regarding its positioning performance.

Alignment stage performance	Chopping stage Performance
Linear range: Z (optical axis), X: $>\pm 8.25$ mm Y (perpendicular to elevation axis): $>+8, -11.5$ mm.	Range: $\pm 1.5$ mrad
Linear incremental accuracy: Z (25 $\mu$ m jump): $<2.5$ $\mu$ m RMS X,Y (100 $\mu$ m jump): $<2$ $\mu$ m RMS	Overall Accuracy ( $R_x, R_y$ ): $<1.6$ $\mu$ rad RMS
Linear overall accuracy: Z: $<10$ $\mu$ m RMS X,Y (100 $\mu$ m jump): $<22$ $\mu$ m RMS	Overall Repeatability ( $R_x, R_y$ ): $<0.48$ $\mu$ rad RMS
Angular range $R_x, R_y$ : $>\pm 1.5$ mrad	Settling Time 0.370 mrad throw: $<20$ ms 2.9 mrad throw $<80$ ms
Angular incremental accuracy (10 $\mu$ rad jump): RMS $<0.52$ $\mu$ rad	<b>Overall Jitter</b>
Angular overall accuracy: $<5.7$ $\mu$ rad RMS	Along Z: $<0.98$ $\mu$ m
Resolution: $<1/10$ of incremental accuracy	Assuming equally distributed contributions: About $R_x, R_y$ $<0.16$ $\mu$ rad Along X, Y $<0.57$ $\mu$ m

Table 1: GTC Secondary Mirror Drives main specifications

\* [egarcia@nte.es](mailto:egarcia@nte.es); NTE, S.A., Can Malé s/n, 08186 Lliça d' Amunt (Spain)

\*\* [lorenzo.zago@csem.ch](mailto:lorenzo.zago@csem.ch); CSEM S.A., Rue Jaquet-Droz 1, CH-2007 Neuchâtel (Switzerland)

\*\*\* [gallieni@ads-int.com](mailto:gallieni@ads-int.com); ADS International, s.r.l., c.so Promessi Sposi, 23/d, 23900 Lecco (Italy)

These specifications must be met for a 46 kg mirror, be kept under wind load conditions, and introduce minimal perturbations on the telescope, both mechanical and thermal. Other significant design constraints are compliance to GTC software and hardware standards, and ensure a high (>99,8%) high-time availability.

The concept developed to meet these requirements consists in a system with two independent stages, namely a Stewart-platform type hexapod to provide alignment, and a fast tilting stage, driven by voice coils and including a passive compensation of the reaction forces.

The overall design of this system has been presented in (1). The present paper highlights some of the key design and development aspects.

## 2. HEXAPOD ACTUATORS

The six hexapod actuators are based on a DC motor-planetary roller screw design. The position feedback is provided by an optical lineal encoder, with a resolution down to 40 nm. An additional rotary encoder directly coupled to the actuator screw readily provides a velocity signal. Nominal axial loads are up to 4000 N, its range  $\pm 17$  mm, and its stiffness 132 N/ $\mu\text{m}$ , yielding a first eigenmode at 155 Hz. Figure 1 shows one of the actuators in the test bench. Dummy flexures, dimensioned to have stiffness and range close to the actual ones, were used along the tests, and can be seen at both extremes of the actuator. The test bench allows loading the actuator in both compression and tension up to 4000N.

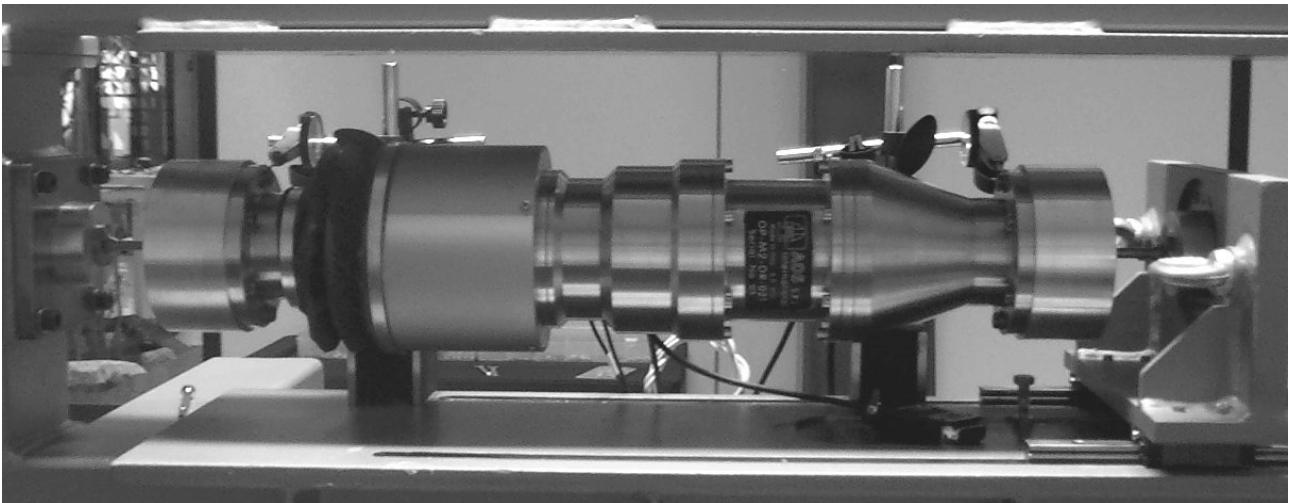


*Figure 1: Hexapod actuators under test*

The actuators are commanded through a PMAC controller. The PID gains were optimized to work under all the loading conditions to assure the control robustness. The use of a “Negative Gain Trap” resulted very effective for what concerns the closed loop in-position stability.

Step response performance is illustrated in figure 2, for a 120  $\mu\text{m}$  step, 4000 N load. The commanded profile has been chosen in order to get about 0.15 s settling time. All the step responses are well shaped. The use of some velocity feed-forward gain allowed canceling the delay typical of large inertia system.

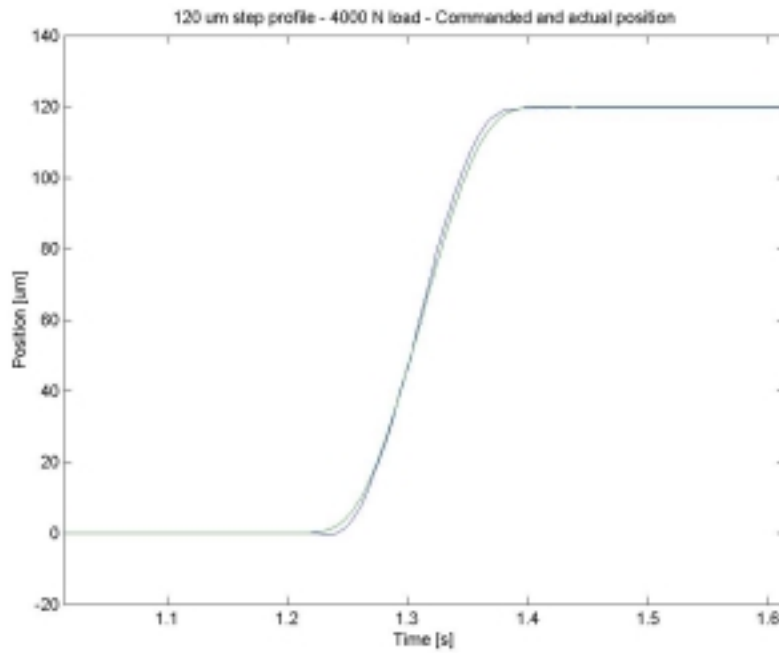


*Figure 2: Hexapod actuator step response*

The theoretically attainable resolution is determined by the linear encoder used, down to 10 nm resolution. However, using this resolution, stable behavior is not attained at normal operating speeds ( $>100 \mu\text{m/s}$ ). Thus, a 40 nm resolution is set, and although it would be possible to change the encoder interpolation to achieve lower ones at smaller speeds, this is not really needed for the application.

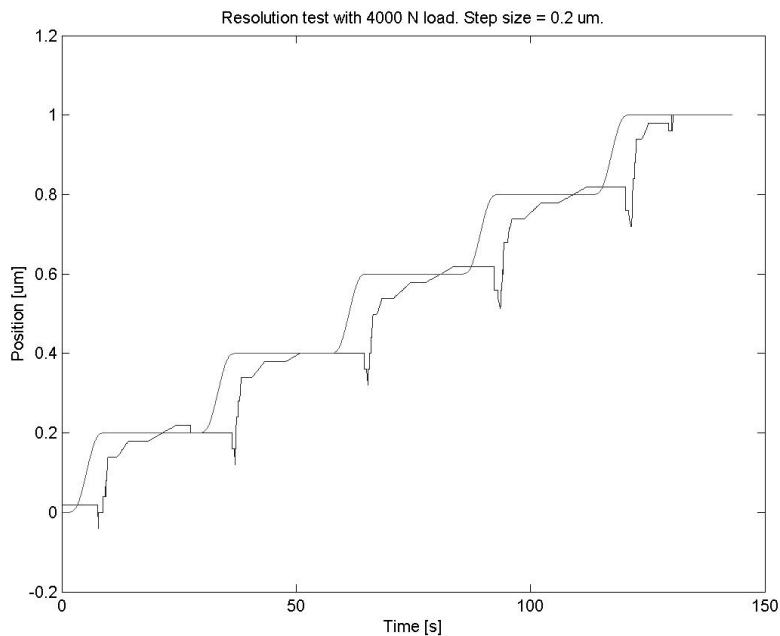


*Figure 3: Resolution test at 4000 N load, 200 nm staircase*

Figure 3 shows the resolution under 4000 N loads, step size 0.2  $\mu\text{m}$ . Position accuracy is always within the commanded encoder count.

The measured standard deviation of the following error (that is, the difference between expected and actual position) is less than 0.5  $\mu\text{m}$ . For zero-speed (that means keeping the commanded position in closed loop), the typical fluctuations are within  $\pm 1$  encoder counts: most of the time the position is perfectly still. Figure 4 shows position, actual speed, and following error for a 0.5 mm/s command, zero load.

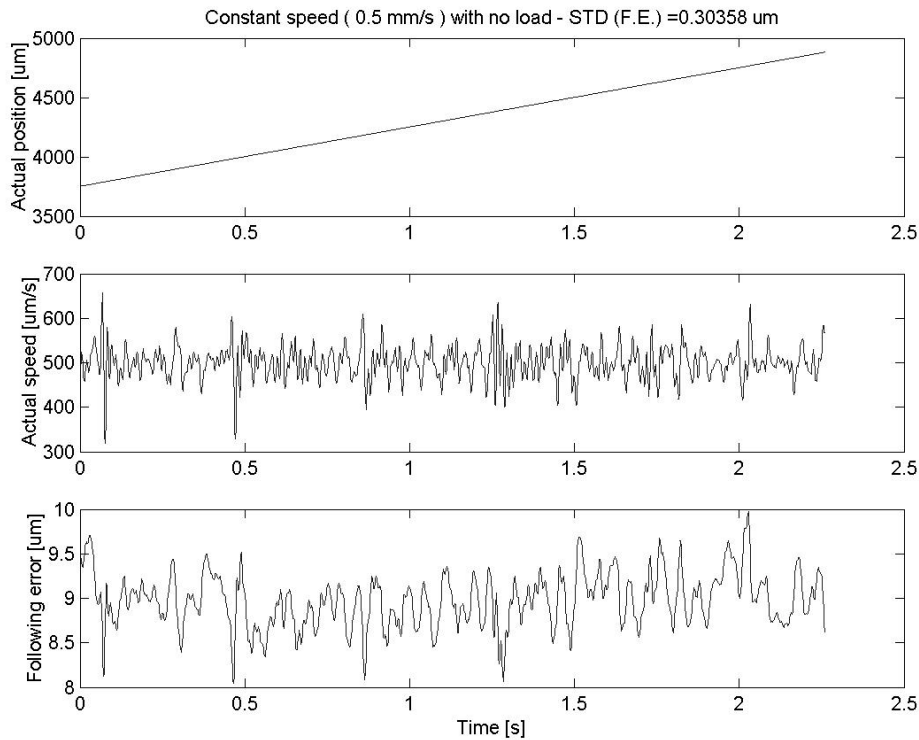


Figure 4: Position, actual speed and following error for 0.5 mm/s, no load

Power consumption as a function of the load, which has an impact on the cooling system design if temperature gradients are to be avoided, was measured to be 0.0023 W/N, plus an additional 2 W for zero load at a 0.5 mm/s speed.

One of the factors to be taken into account when selecting flexure elements for the hexapod is that radial loads are induced in the actuators, in this case on the roller screw. To make sure that this radial load would not introduce any performance degradation due to loss of preload or sizing, one of the actuators was life tested for 15000 cycles, 1000 N axial load, 50 N radial load. Absence of back-slash and compliance with jitter requirements was checked, with satisfactory results, after this testing.

### 3. HEXAPOD FLEXURE JOINTS

One of the key design features is the usage of flexural elements for the hexapod joints. This solution provides repeatable, back-slash free motion, absence of static torque, and no maintenance requirements. Adequately sized according to the operational ranges, their stiffness and fatigue life fulfill the system requirements with comfortable margins. Their main drawback resides in the fact that motion limitation is critical, as unwanted hexapod displacements may lead to excessive stresses, leading to permanent deformation.

To overcome this problem, each of the joints is limited in range to ensure that their flexion does not reach the elastic limit. To this end, the flexures are embedded in two coaxial steel jackets (see figure 5), each of them rigidly attached to both extremes of the flexure. These jackets have internal contact rings to provide an electrical limit switch, so when the contact is closed there is a signal to stop the hexapod actuators. In addition, the current to the motors is limited, and in case of failure of the electrical switch, the increase of current required by the motors to press against the jackets also stops the system.

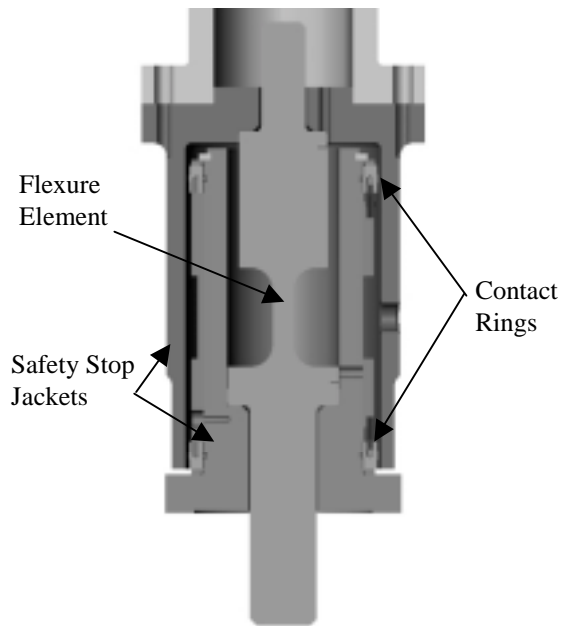


Figure 5: Hexapod flexure joints design

On top of these mechanical and electrical limits, the hexapod motion control calculates the joints' angles for a commanded position, and inhibits the command if any of the expected flexure angles is above the acceptable range. This scheme adds up to a double failure tolerant protection.

The sizing of flexure joints is constrained by two opposing requirements, namely the greatest possible axial stiffness versus the bending stresses in displaced configurations acceptable for the material. Material selection is key to the optimization of these factors. Copper Beryllium alloys, the design choice, offers a low elastic modulus, and high yield strength. The shape is cylindrical, with a 6 mm diameter and 25 mm length. The axial stiffness is thus 150 N/ $\mu\text{m}$ , leading to a 38 Hz hexapod first mode, and maximum operational stress about 533 MPa, being the yield limit of the material 1200 MPa. The safety stops limit the bending to 24 mrad, at which the maximum stress is 750 Mpa.

### 4. LOCKING DEVICES

In order to provide adequate stiffness when the operating mode does not require chopping or fast alignment, and to avoid overstressing the mirror support/reaction mass flexible membranes during integration and maintenance activities, the mirror support can be locked to the hexapod mobile plate.

Figure 6 illustrates the locking devices. A head with two free rotating rollers engages, when needed, into the fixed hexapod plate, providing both vertical and tangential locking. This head is driven by a motor, and loaded with a spring to provide a fail-safe system, that is, in case of power failure the mirror support is automatically locked. The motor, spring and the reduction gear (conical right angle transmission) are selected to provide a minimum continuous power dissipation, since the motor must be continuously powered during chopping stage operation.

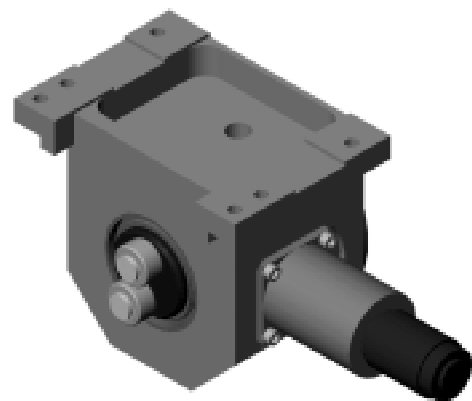


Figure 6: Chopping stage locking device

## 5. COPPER-BERYLLIUM FLEXURE PARTS

Flexural links are used throughout the subsystem in order to reduce friction, back-slash, and wear out, namely:

- Hexapod joints, as described in section 3.
- Chopping stage (mirror support and reaction mass) membranes, which provide the necessary degrees of freedom for the mirror support and reaction mass with respect to the hexapod mobile platform, along the Z (linear along telescope optical axis),  $R_x$  and  $R_y$  (rotations perpendicular to the optical axis) directions, while restraining lateral displacements and rotation about Z axis. Each of the membranes are implemented by means of 16 separate, "I" shaped elements. Sizing of the membranes is critical to achieve a correct balancing of the mirror/mirror support and reaction masses.
- Position sensors heads guidance, which ensure parallelism between the position sensor heads and the rule, and compensate the angular displacement of the sensor bars due to lateral displacements of the drives. The former function is achieved by means of a parallelogram configuration, with flexible sides, while each bar accommodates the deflection by means of two pivots.
- Voice coil actuators guidance, meant to compensate for the angular relative displacement of the mirror support and reaction masses. Again, a parallelogram configuration ensures parallelism of the coil and magnet parts of the voice coil, while pivots accommodate the angle.

All these parts are manufactured in copper-beryllium alloys, due to their elastic and strength characteristics. Dimensionally demanding parts, such as the membranes, are cut from plate by Electro-Discharge Machining, and submitted to a thermal treatment to avoid residual stresses.

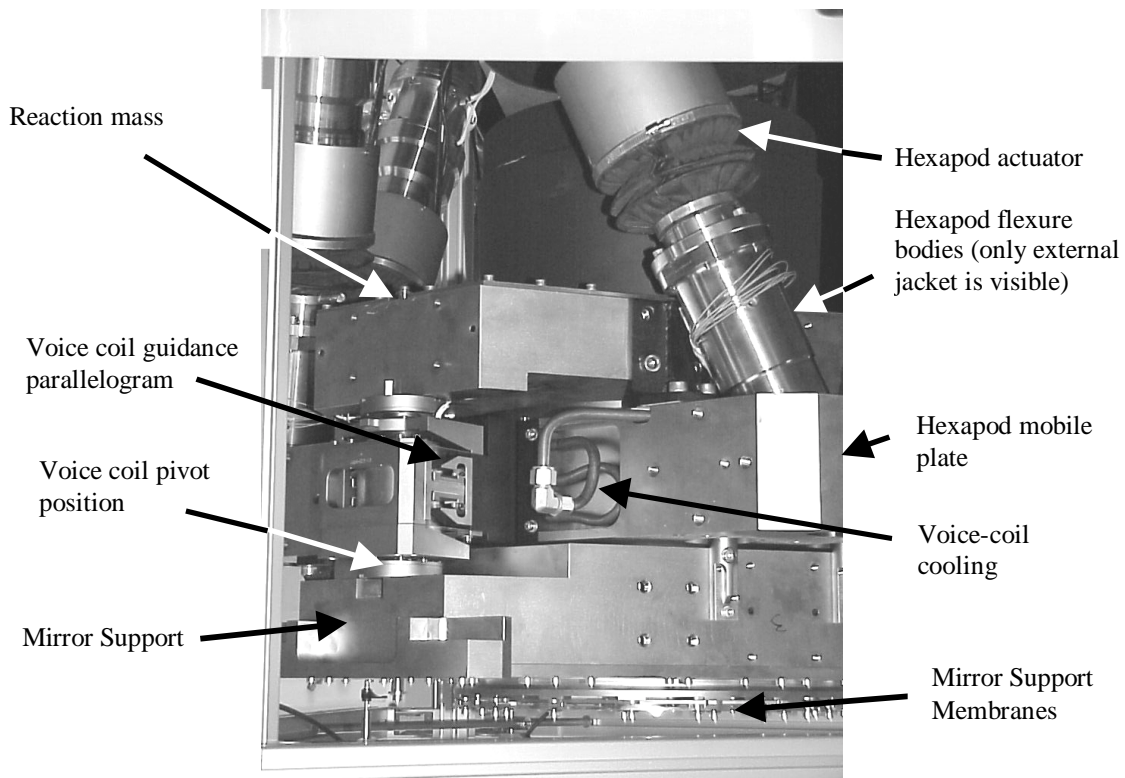


*Figure 7: Flexure element usage*

Figure 7 shows the actual implementation of some of these flexural elements, showing also the current (as of the date of submittal of this paper) status of the integration.

## 6. RAMS ASSURANCE APPROACH

Overall GTC requirements in what regards Reliability, Availability, Maintainability and Safety aspects were apportioned by the Project Office to the different telescope subsystems and specified accordingly, thus allowing an early identification of design constraints, support equipment, and operational needs. The translation of these aspects into a reliable, maintainable and safe design was ensured by applying different techniques, such as Failure Modes Effects and Criticality Analysis (FMECA), and reliability modeling, according to the maturity of the design.

The design factors influenced by this analysis are the physical distribution of parts, and the addition of diagnostic and dismountability features, thus minimizing the time to repair by reducing the failure detection and the need of parts removal for servicing the elements most likely to fail. In what regards safety, critical hazards (that is, those leading to damage to personnel or facilities), and major hazards (those leading to loosing of observation time) identification led to the inclusion of motion inhibits. The analysis results also provided inputs for the definition of the logistics support needs, in terms of spares and skills to be available on site, and the operations manual in what regards both preventive and corrective procedures.

Reliability figures were estimated taking into account an operations scenario of 50 years service life, 15 hours per day of powered-up electronics, four 0-90° and fourteen 45°-90° elevation cycles per day, and 50% of time with chopping at full deflection, 1.25 Hz. The figures of merit for reliability are different according to the type of element considered, namely:

- For mechanical parts subject to wear-out, it is given in terms of the ratio of cycles for 90% reliability (useful life) to the operational cycles according to the defined operations profile.
- Flexural elements, it is given in terms of the ratio of allowed fatigue stress for the cycles considered, to the operational stress, the former obtained from the stress-strain curves of the material used.
- For electronics and sensors, in terms of Mean Time Between Failures (MTBF) as obtained from the manufacturer, or evaluated by similarity to parts of the same complexity and maturity.

The main figures obtained are summarized in table 2:

Based on these figures, the following design features were established in order to optimize the maintainability of the system:

- Electronics, particularly power supplies and power amplifiers, were placed in a readily accessible area, above the hexapod fixed plate. This area can be reached from a dome service platform, tilting the mirror to horizon.
- Voice coils and hexapod actuators can be replaced independently on site, that is, without the need to extract the whole drive system from the secondary spider.
- The maintainability approach is based on limiting the on-site activities to replacement of whole mechanical assemblies (such as voice-coil and sensor assemblies, and hexapod actuators) or electrical off-the-shelf parts, to avoid the need for complex support facilities for diagnosis or adjustment on-site.

In what regards safety, the M2 drives is designed to meet the applicable occupational safety and health legislation, particularly in what regards electrical aspects, usage of hazardous materials, and hazards related to the pressurized cooling circuit. In addition to personnel safety, possible hazards leading to damage of other telescope elements (including the secondary mirror itself) and loss of scientific data were also identified. As a result, a scheme of motion inhibits to ensure its limitation to the nominal, non-hazardous range was designed.

These motion inhibits are placed at three levels, that is, software as a first protection, electrical limit switches, and mechanical hard stops. The motion limits are independent for each of the hexapod actuators (as detailed in section 3), and for the chopping stage on the other. In addition, the mirror support is tethered to the hexapod fixed plate.

<b>Mechanical Items subject to wear-out</b>			
<b>Element</b>	<b>Useful life (90% reliability), ×10<sup>6</sup> cycles</b>	<b>Operational cycles ×10<sup>6</sup> cycles</b>	<b>Useful life / Operational cycles</b>
Actuator roller screws	6	1.5	4
Actuator bearings	16 (99% reliability)	1.5	10.7
Actuator motors	10	1.5	6.7
<b>Mechanical Items subject to fatigue</b>			
<b>Element</b>	<b>Allowed fatigue stress (Mpa)</b>	<b>Maximum Operational Stress (Mpa)</b>	<b>Allowed stress/ Operational stress</b>
Mirror support membranes	540	70	7.7
Reaction mass membranes	540	90	6
Voice coil assembly	540	35	15
Voice coil pivots	215	80	2.7
Sensor membranes	540	20	27
Sensor pivots	215	11	19.5
Hexapod joints, full range	610	533	1.1
Hexapod joints, half range	510	267	1.9
<b>Electrical / electronics parts</b>			
<b>Element</b>	<b>MTBF, ×10<sup>6</sup> hours</b>	<b>Data source</b>	
Local Control Central Processing Unit	0.19	Manufacturer data, accelerated life testing	
Motor Control cards	0.250	Similarity	
Motor Current Amplifiers	0.04	Manufacturer Data	
Time card	0.250	Similarity	
VME crate power supply	0.085	Manufacturer Data @ 25°C	
VME Crate Fan	0.065	Manufacturer Data @ 40°C	
Power Supply	0.15	Manufacturer data @ 25°C	
Power Supply	0.26	Manufacturer data @ 25°C	
Temperature sensors	> 1000	NPRD	
Heaters	> 1	NPRD	
Voice coils	10	NPRD	

Table 2: Reliability estimates

## REFERENCES

1. L. Zago, E. García, "The alignment and fast tilt-chop secondary mirror mechanism of the GTC 10.8-m telescope", SPIE Astronomical Telescope & Instrumentation, 2002 (to be published).